https://doi.org/10.5194/egusphere-2023-1186
Preprint. Discussion started: 14 June 2023

Path length and sediment transport estimation from DEMs of Difference: a signal processing approach

Capito Lindsay[1], Pandrin Enrico[2], Bertoldi Walter[2], Surian Nicola[1], Bizzi Simone[1]

[1] Department of Geosciences, University of Padova, Padova, 35131, Italy

[2] Department of Civil, Environmental, and Mechanical Engineering, University of Trento, Trento, 38122, Italy

Correspondence to: Lindsay Capito (lindsaymarie.capito@studenti.unipd.it)

Abstract. The difficulties of measuring bedload transport in gravel bed rivers have given rise to the morphological method wherein sediment transport is inferred from changes in riverbed elevation and estimates of the distance traveled by sediment, its path length. Because current methods for estimating path length are time and labor intensive, we present a method to estimate path length from repeat digital elevation models (DEMs of difference i.e., DoDs). We propose an automated method to extract the spacing between erosional and depositional sites on the DoD by the application of Variational Mode Decomposition (VMD), a signal processing method, to quantify the spacing as a proxy for path length. We developed this method using flume experiments where bed topography and sediment flux were measured and then applied it to published field data with tracer measurements for validation. Our path length estimates had an error lower than 30% when compared to the measured mode of the tracer distances in the field and generated sediment transport estimates not significantly different than the measured sediment flux at lower discharges in the lab. However, we observed an underestimation of sediment flux at the higher discharges in the flume study. We explore explanations for the underestimation and how the time between survey acquisitions, the morphological active width relative to the channel width, and DoD thresholding techniques affect the proposed method and the potential issues they pose to the morphological method in general.

1 Introduction

In gravel bed rivers sediment transport fundamentally controls morphological processes but is notoriously difficult to measure due to its spatial and temporal heterogeneity (Hoey, 1992; McLean and Church, 1999) measurement uncertainty (Vericat et al., 2006), and the logistical challenges of field measurements. The morphological approach is a method to estimate bedload transport based on observed changes in morphology coupled with an estimate of how far sediment travels, the path length (Ashmore and Church, 1998), or a known flux at one boundary (Grams et al., 2013). With the increasing availability of high-resolution topography, it is now easier to quantify the volume of mobilized sediment needed for the morphological method from the comparison of repeat topographic surveys known as digital elevation models (DEMs) whereby the older survey is subtracted from the newer survey to obtain a DEM of difference (DoD). However, the estimation of path length remains a challenge.

Implementation of the path length-based approach requires an estimation of typical particle travel distances for the reach in question. Historically, these distances have been estimated using tracers, either electronically tagged or painted clasts. Unfortunately, tracer studies are time and labor intensive, requiring multiple site visits and intensive recovery campaigns which often have low recovery rates, especially for painted clasts (Hassan and Bradley, 2017; Brenna et al., 2019). Furthermore, tracer studies are often applicable only to exposed bars, ignoring a large portion of in-channel transport, and can be sensitive to the seeding location (Liébault et al., 2012). To overcome these limitations, several methods have been proposed to estimate path length based on the connection to morphology.

https://doi.org/10.5194/egusphere-2023-1186
Preprint. Discussion started: 14 June 2023

Given that morphological units are the cumulative result of the displacement of sediment particles, it follows that the two would be related. Neill (1971) proposed that path length in meandering rivers should be equal to the distance from an erosional site (eroding bank) to the next depositional site (point bar) downstream. Many others have observed similar relationships based on the spacing of erosional and depositional sites and channel morphology (Beechie, 2001; Hundey and Ashmore, 2009; Kasprak et al., 2015; Pyrce and Ashmore, 2003b, a; Vázquez-Tarrío et al., 2019). A synthesis of tracer studies demonstrated that at formative discharges, particle path length distributions often exhibit primary or secondary modes corresponding to the location of bars, where deposition occurs (Pyrce and Ashmore, 2003a). Further, depositional areas (typically bars), have demonstrated a higher probability of 'trapping' particles than erosional morphological units (McDowell and Hassan, 2020; McDowell et al., 2021). Finally, experimental research has confirmed the preferential deposition of particles specifically at bar heads and margins even in channels with more complex morphology, for example, in braided rivers (Kasprak et al., 2015) but it is reasonable to assume that in multithreaded channels, multiple path lengths might exist at different flow stages in primary and secondary channels.

Given the observations linking path length to morphology, we hypothesize that path length can be inferred from changes in morphology at near event scale comparisons. If during a flood, sediment is mobilized from an area of erosion to an area of deposition as represented on the DoD, the distance between the two should correspond to a typical path length. Following this hypothesis, this work has the following objectives: i) to propose an efficient and semiautomatic method to quantify the distance between sites of erosion and deposition from the DoD; ii) to use these estimates of path length to explore the feasibility and accuracy of sediment transport flux estimations, using direct measurements at the laboratory scale; iii) to compare these estimates to measured path lengths obtained from tracer data in the field; iv) and finally to evaluate the potential sources of error when estimating sediment flux from changes in morphology.

2 Methods

To meet our objectives, we use flume experiments at varying discharges with direct measurement of output sediment flux and sets of repeat DEMs from which DoDs are created and used to identify patterns of erosion and deposition. We then develop a semiautomated method to extract these distances between erosion and deposition and compare our estimates to measured sediment flux. Finally, we test this method using published field data with tracer measurements as validation of the path length estimates.

2.1 The morphological method

The morphological method is based on the sediment continuity equation.

$$(Q_{b_{in}} - Q_{b_{out}})\Delta t = (1-p)\Delta V \quad (1)$$

Where $Q_{b_{in}}$ and $Q_{b_{out}}$ are the volumetric sediment flux in and out of the reach respectively, Δt is the time between surveys, p is the sediment porosity, and ΔV is the change in volume. The sediment continuity equation can be solved in several ways, one requires that either the incoming flux $Q_{b_{in}}$ or the outgoing flux $Q_{b_{out}}$ be defined. This has been estimated by setting a zero-flux boundary, such as a dam or gravel sand transition (McLean and Church, 1999), by segmenting the reach such that a zero-flux boundary is set between a section of net deposition to one of net erosion (Vericat et al., 2017) or by measuring flux either into or out of the reach (Grams et al., 2013).

https://doi.org/10.5194/egusphere-2023-1186
Preprint. Discussion started: 14 June 2023

Alternatively, Eq. (1) can be modified so that the virtual velocity, v_b is used.

$$v_b = \frac{L}{T} \tag{2}$$

Where L is the distance the particles travel and T is the time over which the particles are traveling. Vericat et al. (2017) proposed an equation to use the path length with the volume of erosion derived directly from the DoD

$$Q_b = (v_b \sum V_e (1-p)\rho_s)/L_c \tag{3}$$

Where $\sum V_e$ is the total volume of erosion from the DoD and L_c is the length of the analyzed DEM by which the volume of erosion is normalized (Vericat et al., 2017). To use this method, L_c must be long enough for average path lengths (L) to occur and T must be short enough to prevent repeated erosion and deposition, known as compensation (Lindsay and Ashmore, 2002).

2.2 Path length

The crux of our hypothesis is that sediment moves from an area of net erosion to an area of net deposition during the time period between DEM acquisitions and that this represents a characteristic path length. The most obvious method to quantify this distance between erosional and depositional sites on the DoD is to measure the spacing manually using a GIS program however, this requires many subjective evaluations. Firstly, we must decide where on the patches of erosion and deposition to begin and end the measurements. Because patches of erosion and deposition are not symmetrical or of equal size, the distance between the two depends on which area of the patch we choose to begin and end the measurements (Fig. 1). For consistency, we choose the center of the patch (Fig. 1c). Next, we must determine which patch of erosion matches with which patch of deposition which is not always obvious, especially when multiple channels are present, and again requires subjective evaluation. Here we used our knowledge of morphological processes to make a best estimate. For example, a patch of erosion on an outside bend likely corresponds to the deposition of the next point bar downstream. Although this method is capable of producing estimates of path length, to overcome the subjectivity and time required to manually measure the distances we developed a method to extract the spacing that is objective and semiautomated.

https://doi.org/10.5194/egusphere-2023-1186
Preprint. Discussion started: 14 June 2023

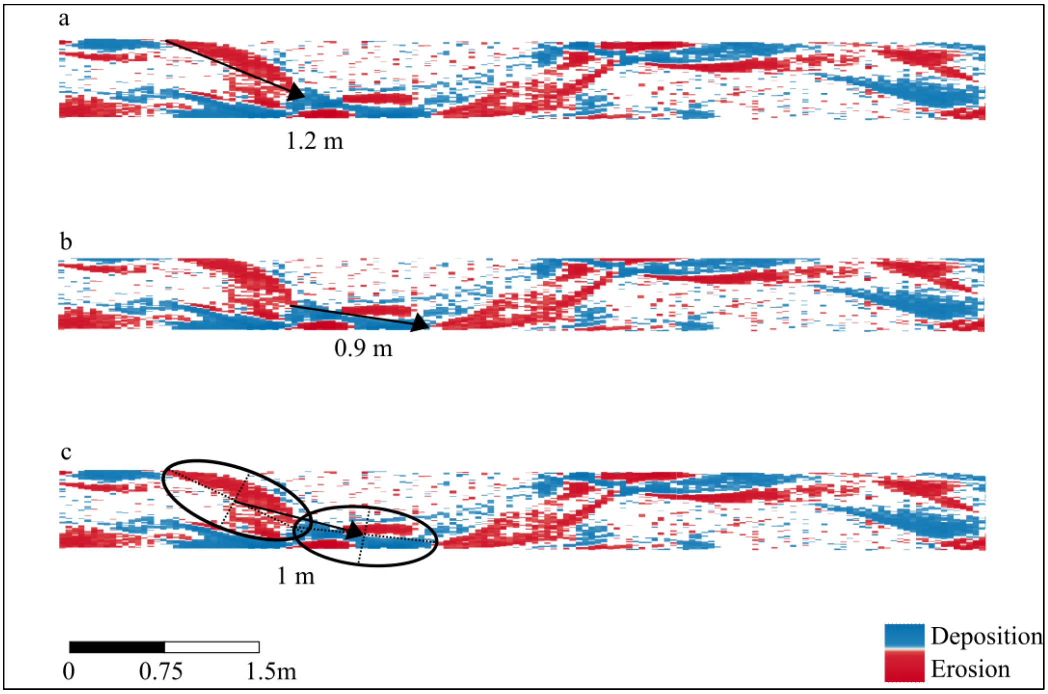

Figure 1: Manual method to measure spacing of erosional patches (red) and depositional patches (blue) on a DoD. (a) Beginning of patch to beginning of next patch (b) end to end (c) center to center.

2.3 Semiautomated extraction of path length

To visualize and then quantify the spacing of erosional and depositional sites on the DoD we simplify the spatial heterogeneity of the DoD into a vector of the net change in elevation in a streamwise direction (Fig. 2a). Because natural rivers are rarely straight, for field case studies, we must enforce a linear downstream directionality essentially straightening the bends in the river. This is achieved by segmenting the DoD into a series of equally sized “bins” using the segmentation tool of the Fluvial Corridor Toolbox (Roux et al., 2015) (Fig. 2a). We then sum the values in each bin to obtain a vector of the net change in elevation in a streamwise direction (Fig. 2b). In the flume studies, where there is no sinuosity, we simply sum each column of the DoD matrix. Oftentimes a reach is aggrading or incising and therefore the net vector will have an increasing or decreasing trend (Fig. 2b). Because we are interested in the spacing between areas of erosion and deposition rather than the overall trend, we remove it by subtracting a best-fit linear trend from the net vector (Fig. 2b).

https://doi.org/10.5194/egusphere-2023-1186
Preprint. Discussion started: 14 June 2023

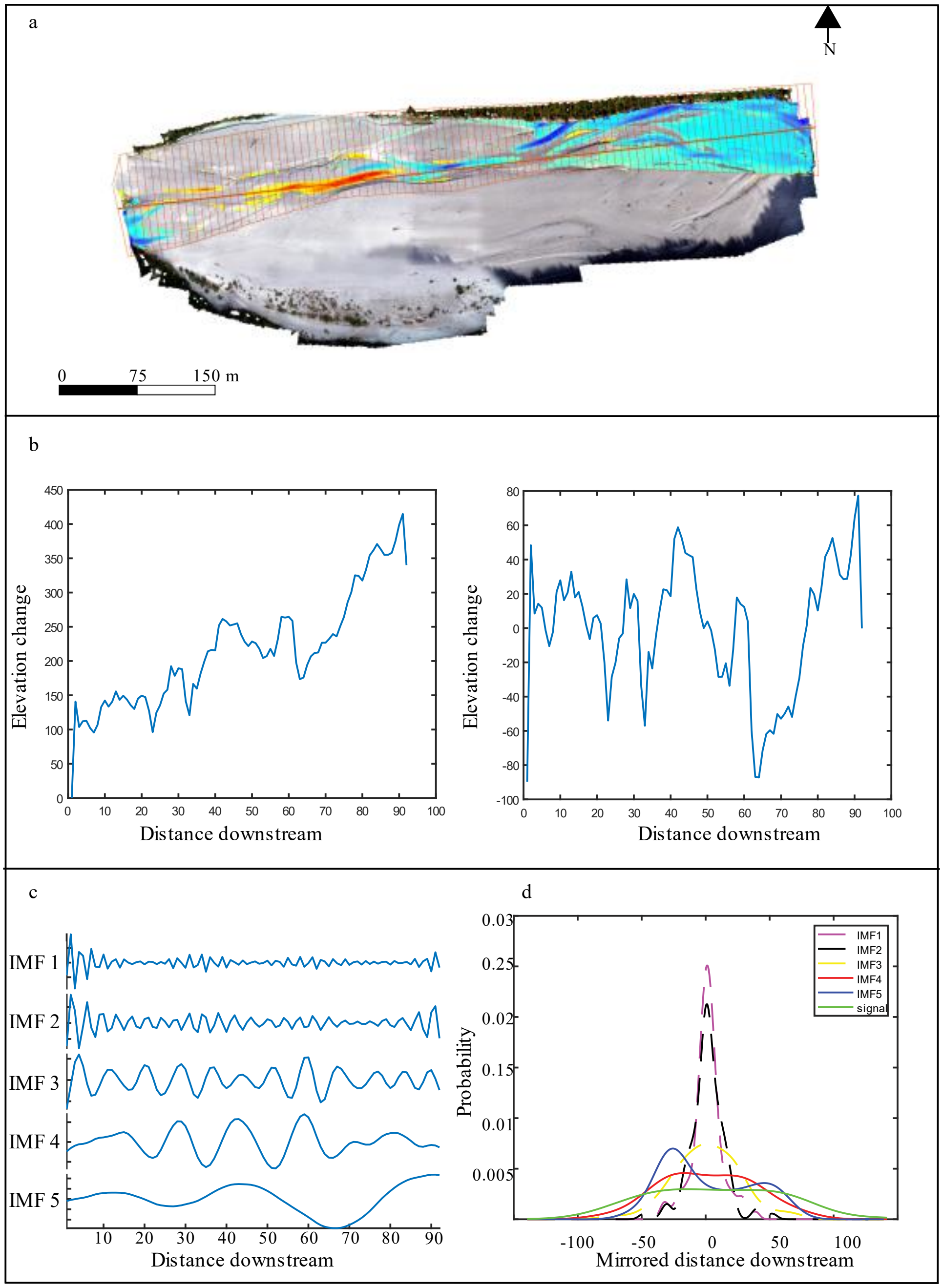

Figure 2: VMD- HD method (a) Segmentation of the DoD. (b) Plot of the net original and detrended vector. (c) Variational mode decomposition (VMD) with 5 intrinsic mode functions (IMFs). (d) Probability density function (PDF) of each IMF and the original net vector.

From Fig.2b, it is clear that the pattern of erosion and deposition exhibits periodicity but there is also variation and “noise”. To see the pattern more clearly and quantify the periodicity we turn to the field of signal processing where the

https://doi.org/10.5194/egusphere-2023-1186
Preprint. Discussion started: 14 June 2023

problem of de-noising is ubiquitous. There are many approaches to de-noising including Fourier transform, empirical mode decomposition (EMD), and wavelet analysis. We chose to use variational mode decomposition (VMD) due to its robustness with respect to sampling and noise (Dragomiretskiy and Zosso, 2014; Huang et al., 2016; Ma et al., 2017). VMD decomposes the signal into a set of intrinsic mode functions (IMFs) each with a different central frequency (Dragomiretskiy and Zosso, 2014; Ma et al., 2017) (Fig. 2c). In this case of our static 'signal' the frequency is more accurately described as the wavelength. It is beyond the scope of this paper to describe the mathematics of VMD in detail, therefore, for a complete explanation see (Dragomiretskiy and Zosso, 2014; Huang et al., 2016; Ma et al., 2017; Upadhyay and Pachori, 2015). Once the original vector is decomposed into the various IMFs, we need to select the IMF or IMFs that most accurately represent the periodicity of the original data. Ma et al. (2017) proposed a method to select the most relevant IMF, and therefore periodicity of the signal, by computing the probability density function (PDF) using kernel density smoothing for each of the five IMFs and of the original data vector (Fig. 2d), then to calculate the Hausdorff distance (HD), a metric of geometric similarity, between each IMF's PDF and the PDF of the original data and select the IMF most geometrically similar to the original data (Ma et al., 2017) (hereafter VMD-HD method). In most cases, the longer wavelength IMFs most closely resemble the original signal whereas the IMFs with shorter wavelengths are more likely associated with noise (Boudraa et al., 2005). The computed wavelength is converted to a meaningful physical quantity by multiplying by the bin spacing in meters. Because we are interested in the distance from peak to trough, we divide the period by two to obtain the path length proxy (Neill,1971; Ashmore and Church, 1998). All calculations were performed in MatLabR2020b.

3 Flume and field data

The method was tested using data from a set of runs performed in the Hydraulic Laboratory of the University of Trento, where DEMs were generated for fixed time intervals and varying discharges, and direct measurements of the bedload flux were also collected. To test the efficacy of the method in the field, we selected a published dataset of measured path lengths with corresponding DoDs for the San Juan River in British Columbia Canada (McQueen et al., 2021). In this case, DoDs and corresponding tracer data were available for three separate bars (bar 6, bar 7, and bar 15) for the 2018-2019 period. Detailed information on their collection and processing can be found in McQueen et al., 2021.

3.1 Flume experiments

The Trento laboratory experiments were carried out in a 0.6 m wide and 24 m long flume, filled with sand characterized by a median diameter (D_{50}) of 1 mm. The flume slope was set to 0.01 m/m. Topographic surveys were performed over the final 14 m of the flume, to limit the upstream inflow effects, using a laser gauge, mounted on a movable deck. The longitudinal and crosswise spacings were 0.05 m and 0.005 m, respectively. Four sets of runs were performed, with the flow discharge set to 0.7, 1, 1.5, and 2 l/s, which correspond to a range of different planform morphologies (see Fig. 3). The runs were performed following the same procedure, involving three phases of different lengths, based on the transport condition of each discharge. These durations were estimated referring to the time scale for morphological evolution computed from the sediment balance mass equation (Garcia Lugo et al., 2015), which can be expressed as:

$$T\_ex = \frac{DW^2}{Q_b}, \quad (4)$$

where D is the average flow depth and W is the flow width. Table 1 provides the values of T_ex for each flume experiment.

Table 1: Initial conditions for each dataset including the type of validation data.

https://doi.org/10.5194/egusphere-2023-1186
Preprint. Discussion started: 14 June 2023

	Flume 1	Flume 2	Flume 3	Flume 4	San Juan Bar 6	San Juan Bar 7	San Juan Bar 15
Peak discharge (m^3/s)	0.0007	0.001	0.0015	0.002	942	942	942
Slope (m/m)	0.01	0.01	0.01	0.01	0.0038	0.0031	0.0009
Width (m)	0.6	0.6	0.6	0.6	150	150	130
D_{50} (m)	0.001	0.001	0.001	0.001	0.05	0.056	0.042
Time scale T_ex (min) (eq.4)	94	50	38	30	-	-	-
Time between surveys (0.5 T_ex)	47	25	19	15	1 year	1 year	1 year
ω* Dimensionless stream power	0.15	0.22	0.33	0.43	0.76	0.61	0.31
Validation Data	Sediment Flux	Sediment Flux	Sediment Flux	Sediment Flux	RFID tracers	RFID tracers	RFID tracers

First, an initial phase of about 12 times this time scale T_ex with constant flow was run, to ensure the formation of a near-equilibrium morphological condition, starting from a flat sand bed scraped to the prescribed slope. This was followed by a long run, at constant discharge, lasting 19 times the time scale T_ex, aimed at measuring the output sediment flux. This was continuously monitored at the channel outlet, through a permeable basket placed on four load cells. Sediment flux was measured every minute. After a bed topography survey, the third phase was a sequence of nine shorter runs, lasting 0.5 times the time scale T_ex, each followed by a bed topography survey, which produced nine corresponding DoDs. The duration of these nine runs (and therefore the time interval between surveys) was decided to have easily measurable changes of the bed morphology, without having significant compensation processes. The use of the time scale T_ex (and therefore a different absolute time interval between surveys for the four discharges) ensured to have similar volumes of erosion and deposition in each run.

The DoDs were created by subtracting two consecutive DEMs, then underwent a three-step filtering process to highlight the relevant erosion and deposition patterns, removing most of the noise associated with the surface roughness and measurement accuracy. First, the DoDs were filtered considering a uniform detection threshold equal to 2 mm (2 times the D_{50}), meaning that erosion or deposition values lower than this threshold are set to zero. Thereafter, a spatial average was performed as a moving average on three values along the transversal direction where the DoD discretization is the finest. Lastly, a despeckling algorithm removed all isolated cells, both considering single cells that show erosion or deposition, as well as single cells that show no change. This last step was implemented to keep the detection threshold as low as possible while removing unphysically small areas. Additionally, we calculated the morphological active width by determining the percentage of the DoD that showed morphological activity (i.e., was not zero after filtering).

3.2 San Juan River data

The San Juan River DoDs were downloaded directly from the Scholars Portal Dataverse (https://doi.org/10.5683/SP2/UQGZCG). The time in between acquisitions is one year, in which it is estimated there were five flood events able to generate sediment transport using a threshold of 500 m3 s−1, which was visually estimated by the authors to be equivalent to the bankfull discharge (McQueen et al., 2021). DEMs were generated by LIDAR acquisitions and have a spatial resolution of 10 cm and a vertical root mean square error lower than 10 cm. Topographic changes between survey dates were then calculated by processing the LiDAR DEMs using the Geomorphic Change Detection (GCD) software (Wheaton et al., 2010). More information on how they were obtained and processed including the spatially variable thresholding techniques can be found in McQueen et al., 2021. The

https://doi.org/10.5194/egusphere-2023-1186
Preprint. Discussion started: 14 June 2023

LiDAR-derived DoDs were used to interpret patterns of tracer displacement and burial depths and to provide information on the morphological development of the bars during the study period. However, they do not provide complete reach-scale sediment budgets due to the lack of in-channel topographic data and stage differences during each LiDAR survey affecting the relative portion of the river bed that was exposed. Nevertheless, we believe the exposed part of the channel, the bars, and associated patches of erosion and deposition (see Fig. 8b) are sufficient to be used with our proposed method to estimate path lengths and be compared with field measured path lengths from the tracer data.

3.3 Validation data

Each study had unique initial conditions including slope, discharge, grain size, channel configurations, and time/flood events between surveys (Table 1). Because the studies vary with respect to these initial conditions, we calculated the dimensionless stream power (ω*) after Bertoldi et al., 2009 to compare them.

$$\omega^* = \frac{Q \cdot S}{W\sqrt{g \Delta D_{50}^3}} \tag{5}$$

Where Q is the peak discharge, S is slope, W is the average wetted width, Δ is the relative submerged density, D_{50} is the median grain size, and g is the acceleration due to gravity.

For the flumes, we used estimates of path length generated by the VMD-HD method to calculate the virtual velocity Eq. (2) and sediment flux Eq. (3) which we then compared to measured flux data. The measured sediment flux during the initial long run showed high variability, with phases of high and low sediment flux lasting several tens of minutes. For this reason, we prefer to use the data from the long runs, from which we estimated an average sediment flux of 0.33 g/s (SD=0.17) for the 0.7 l/s discharge, 0.78 g/s (SD=0.31) for the 1 l/s discharge, 1.98 g/s (SD=0.65) for the 1.5 l/s discharge, and 3.22 g/s (SD=0.79) for the 2 l/s discharge (Fig. 3). We subdivided the second phase into 38 intervals of 0.5 *T_ex* duration, equal to the duration as the short runs in phase 3, and computed the variability of the flux over this range.

We used ANOVA to compare path length, virtual velocity, and erosion across the four discharges (α=0.05) and a Post-hoc Tukey test to explore significant differences between discharges. To compare the measured sediment flux to the estimates from the VMD-HD method we used a student's t-test (α=0.05). And finally, to compare the error of our path length and sediment transport estimates we calculated the symmetrical mean absolute percent error (SMAPE).

For the San Juan River we compared the VMD-HD estimates of path length to the published path length distributions. The tracer recovery locations were accessed in spreadsheet form and in keeping with the analysis of the authors we disregarded any tracers that moved less than 10 m before calculating the path length distributions.

4 Results

4.1 Flume experiment

To aid in the interpretation of the results, Fig. 3 shows a DoD from each of the discharges with the IMF 5 vector laid over the top. Oftentimes the areas of deposition and erosion from the DoD correspond clearly to the IMF 5 vector as with the 0.7 l/s discharge where areas of deposition are concave and areas of net erosion correspond to convex areas of the vector. At the higher discharges (1.5 l/s and 2 l/s) the total area of morphological activity increases and patches of erosion and deposition begin to overlap, creating a more chaotic and difficult to discern pattern (Fig. 3).

https://doi.org/10.5194/egusphere-2023-1186
Preprint. Discussion started: 14 June 2023

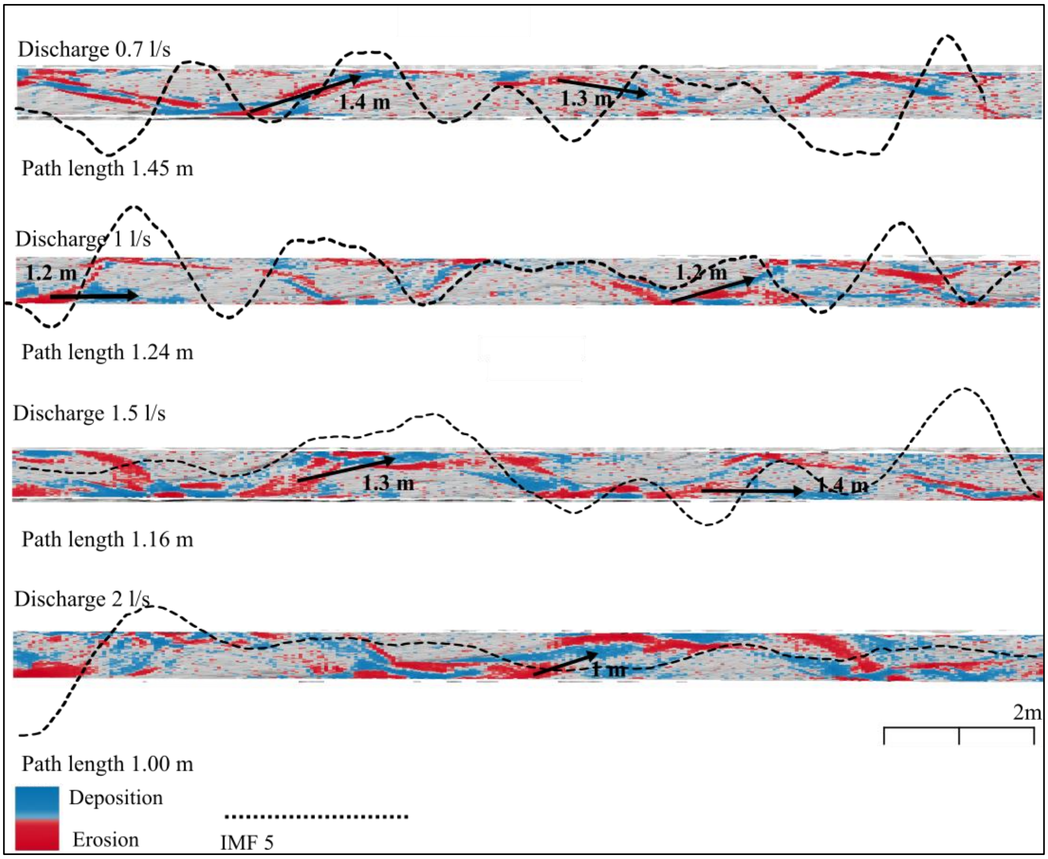

Figure 3: All four discharges from the flume experiment DoDs with arrows showing manually derived distances from erosion to deposition, path length estimates using the VMD-HD method, and the IMF 5 vector.

In the flume experiment, the VMD-HD method of choosing the most relevant IMF selected the longest wavelength IMF 5 74% of the time and IMF 4 34% of the time. IMFs 2 and 3 were never selected and IMF 1 was selected only once. Using the selected IMFs, the method estimated a similar average path length for all of the discharges (Fig. 4 & 5). The averages were, 1.45 m (SD = 0.93) for the 0.7 l/s discharge runs, 1.24 m (SD=0.58) for the 1 l/s runs, 1.21 m (SD = 0.58) for the 1.5 l/s runs, and 1 m (SD = 0.37) for the 2 l/s runs (Fig. 3). The path length estimates derived from the VMD-HD method matched closely with the manually measured distances and there were no statistically significant differences for any of the discharges (p-value > 0.05) (Fig. 4).

https://doi.org/10.5194/egusphere-2023-1186
Preprint. Discussion started: 14 June 2023

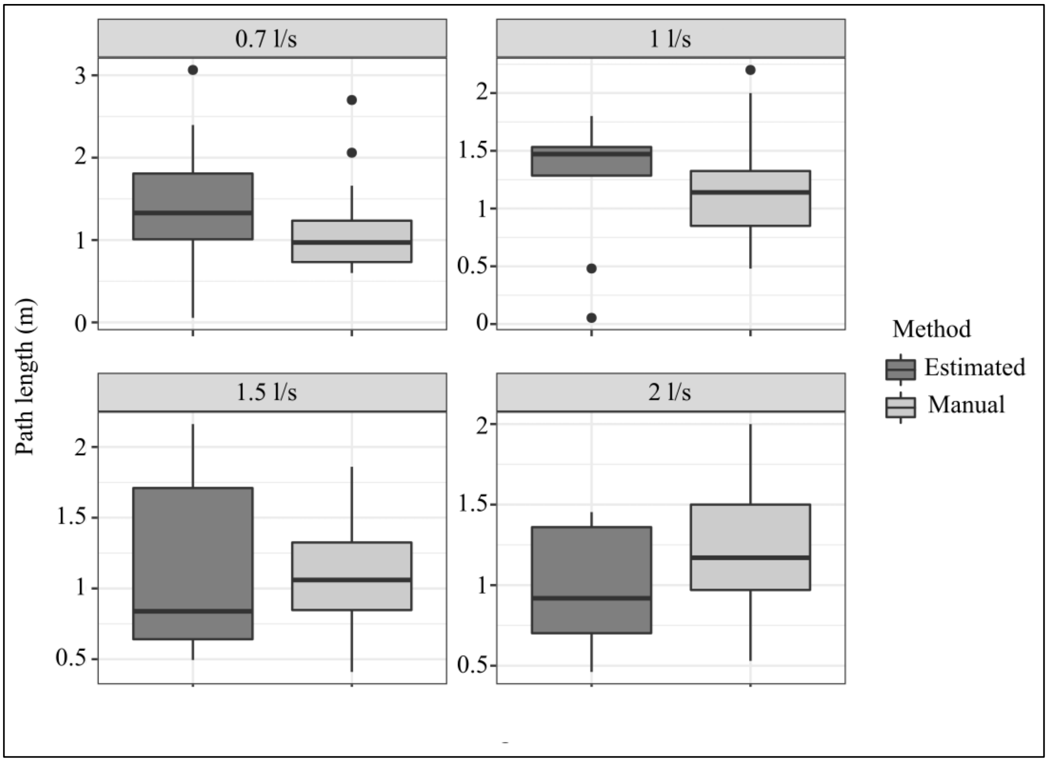

Figure 4: Path length estimates from the VMD-HD method (dark gray) and the estimates derived from the manual method (light gray). The two groups were not statistically significant (p-value > 0.05).

The estimated path lengths were not significantly different between the discharges (p-value >0.05) (Fig. 5) and showed no obvious trend of increasing or decreasing with discharge. However, when used to calculate the virtual velocity (v_b) wherein the path length is divided by the time between surveys (Table 1), we see an increase in the virtual velocity with discharge (p-value < 0.05) (Fig. 5). Likewise, the average volume of erosion calculated from the DoDs increases significantly with discharge (p-value < 0.001) (Fig. 5).

https://doi.org/10.5194/egusphere-2023-1186
Preprint. Discussion started: 14 June 2023

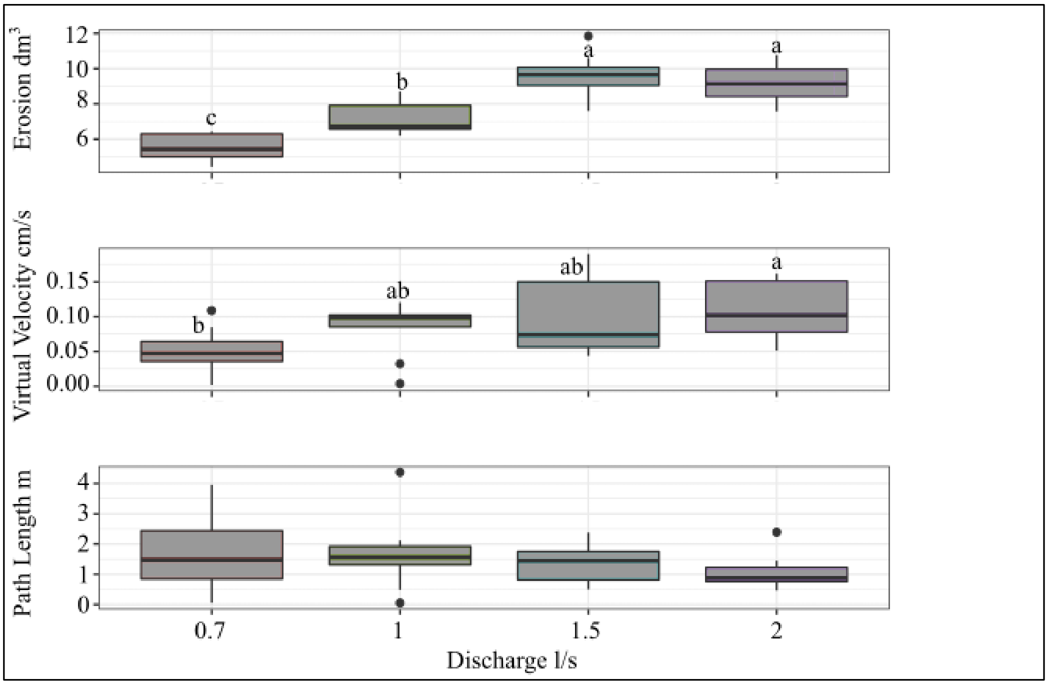

Figure 5: Estimated path length using the VMD-HD method for all discharges in the flume experiment, calculated virtual velocity using these estimates, and measured volumes of erosion. Significant differences from the Post hoc Tukey test are denoted by letters a-c.

When used to calculate sediment transport Eq. (3) the VMD-HD method corresponds well to the measured average for the lower discharges (0.7 l/s and 1 l/s) whereas at the higher discharges (1.5 l/s and 2 l/s) the method significantly underestimated the measured flux (Fig. 6). For the 0.7 l/s discharge, the VMD-HD method estimated a rate of 0.39 g/s (SD = 0.25) averaged over the nine runs, which was not significantly different than the measured average of 0.33 g/s (SD = 0.18) and the SMAPE was 4%. For the 1 l/s discharge the method estimated 0.81 g/s (SD = 0.38) and was not significantly different than the measured average of 0.78 g/s (SD= 0.30) with a SMAPE of 11%. At the higher discharge of 1.5 l/s the average estimated by the VMD-HD method was 1.21 g/s (SD = 0.47) whereas the measured average was 1.98 g/s (SD = 0.70) (p-value < 0.05) with a SMAPE of 53%. Finally, for the 2 l/s runs the estimated average was 1.44g/s (SD = 0.46) whereas the measured average was 3.22 g/s (SD = 0.98) (p-value < 0.001) (Fig. 6) with an SMAPE of 90%.

https://doi.org/10.5194/egusphere-2023-1186
Preprint. Discussion started: 14 June 2023

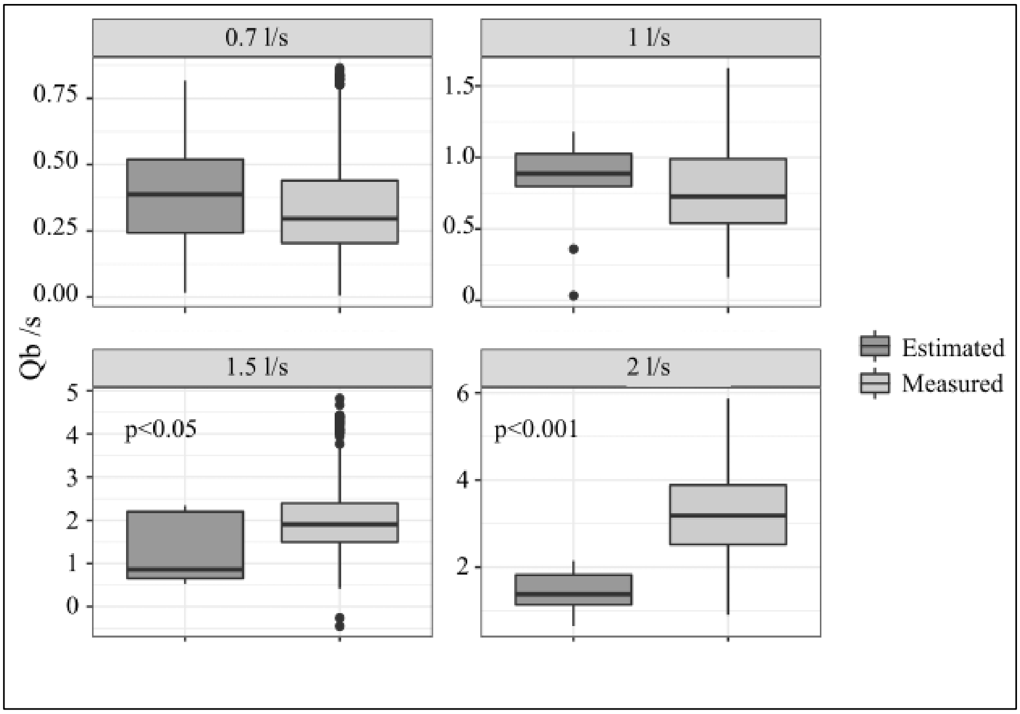

Figure 6: Estimated sediment flux (dark gray) compared to the measured average (light gray) for each of the 4 discharges from the flume experiment. Significant p values (α<0.05) from a student's t-test are shown for the 1.5 l/s and the 2 l/s discharges.

4.2 San Juan River

For the three bars in the San Juan River dataset, the path length calculated from the VMD-HD method for bar 6 was approximately 217 m whereas the field measured average from tracers was 153 m (SMAPE=35%), and the mode range was 150-200 m. For bar 7 the method calculated a path length of 324 m whereas the measured average was 255 m (SMAPE=24%), and the secondary mode range was 280-380 m. Finally, for bar 15 the method calculated a path length of 323 m whereas the measured average was 221 m (SMAPE=38%), and the secondary mode range was 200-300 (Fig. 7).

https://doi.org/10.5194/egusphere-2023-1186
Preprint. Discussion started: 14 June 2023

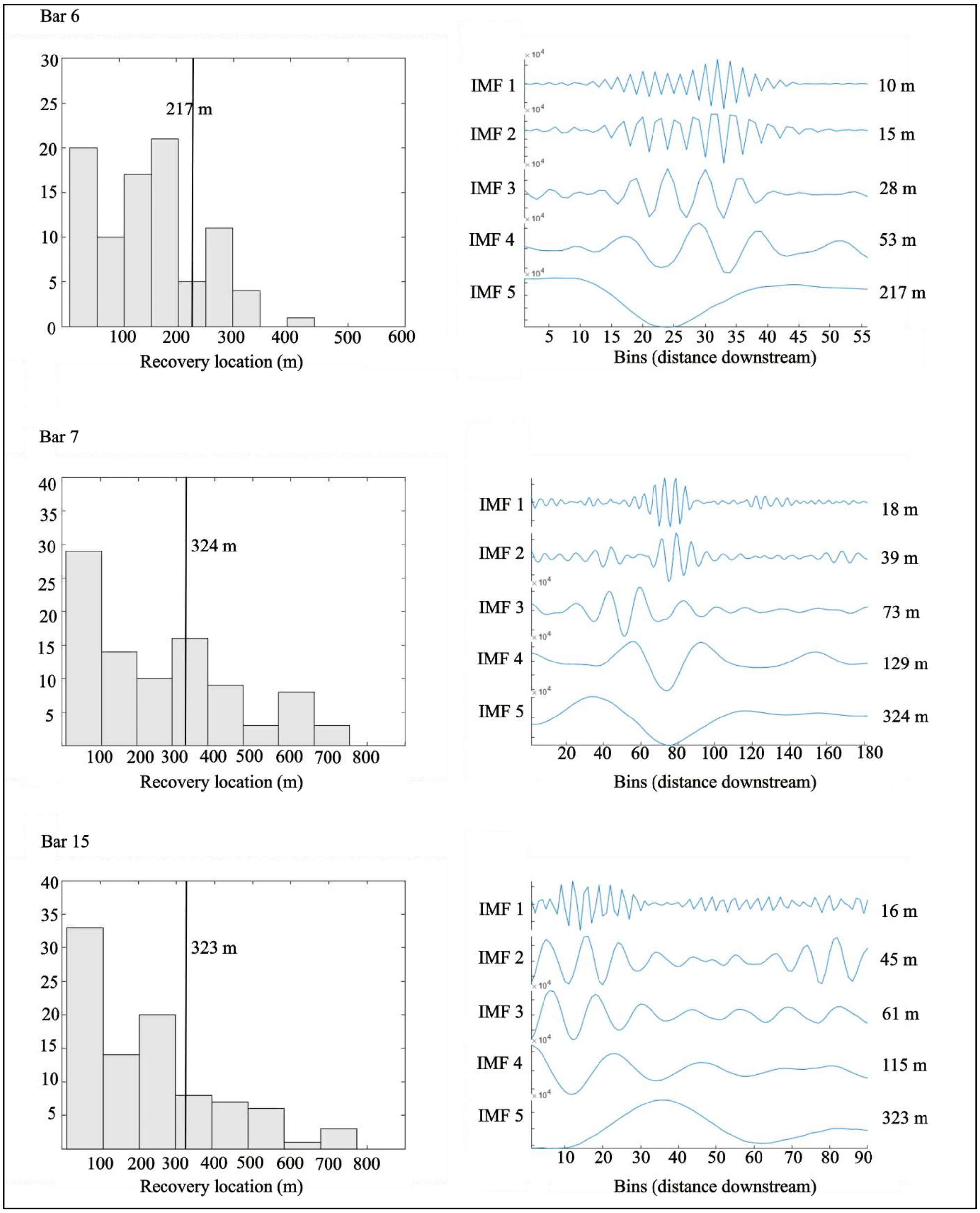

Figure 7: Tracers-based path length distributions (on the left) and VMD derived IMFs for bars 6,7, and 15 from the San Juan River dataset. The VMD-HD method selected IMF 5 for all three bars and is reported on the histograms on the left for visual comparison.

5 Discussion

We developed a method to estimate the representative path length during a given flood using information inherent to the DoD by applying the principle that at channel-forming flows, the majority of particles move from an area of erosion to the next area of deposition downstream (Pyrce and Ashmore, 2003b, a). Therefore, we hypothesized that the distance between net erosional and depositional sites should provide a reasonable estimate of the path length. Our method

https://doi.org/10.5194/egusphere-2023-1186
Preprint. Discussion started: 14 June 2023

overcomes the subjectivity and time involved in measuring these distances manually while aligning closely with these manually measured distances (Fig. 4). Further, our estimates have an error lower than 30% when compared to the measured mode of tracer-derived path length estimates in the field (Fig. 7). When used to calculate sediment flux our estimates are not significantly different than direct measurements of sediment flux for the lower discharge ranges in the lab (Fig. 6). Importantly, we observed that the method underestimates the sediment flux significantly for the two highest discharges in the lab where the bed shows a higher percentage of topographic change (Fig. 6). The method presented to estimate path length using only remotely sensed data shows promising results under certain conditions and provides insight into conditions where it is not applicable.

5.1 Path length estimation by VMD-HD method: limitations and perspectives

Previous studies have shown a relationship between path length and hydrologic variables such as discharge, stream power, and excess shear stress (Hassan et al., 1991; Pyrce and Ashmore, 2003b). A notable result of the flume experiment is that the estimated path length did not significantly differ between the four discharges (Fig. 4 & 5). We propose two possible explanations for this discrepancy with the literature. First, it is possible that the actual path length is increasing with discharge as has been observed in previous studies (Hassan et al., 1991; Pyrce and Ashmore, 2003b) but the method fails to capture it because the VMD-HD method is based on the spacing of erosion and deposition which does not change for the varying discharges under the flume conditions. It is possible that at higher discharges the characteristic path length is not equal to the spacing of erosion and deposition because the particles are moving farther than the next depositional site downstream. For instance, if we double the estimated path length, hypothesizing a sediment is not trapped in the first depositional area but in the second one, we more closely estimate the sediment transport at the higher discharges (i.e., estimates are not significantly different than the measured averages ($p>0.05$) but overestimate the sediment transport at the 0.7 l/s and 1 l/s discharges ($p<0.05$) (Appendix Fig. A1). A second explanation is that the actual path length does not change with the increase in discharge because the channel width and morphological unit spacing exert a stronger control than any hydrologic variable which has also been observed in previous studies (Beechie, 2001; Pyrce and Ashmore, 2003b; Vázquez-Tarrío et al., 2019). The width may exert an outsized effect in this case because the flume is laterally confined and unable to widen in response to an increase in discharge. Because we do not have tracer data in the flumes for comparison, we can only rely on the sediment transport measurements for validation which indicate that we are underestimating the sediment transport at higher discharges, thus supporting the first explanation, but further flume studies with both sediment flux and tracer data for validation could help resolve this question.

The VMD-HD method presented here selects one of the five IMFs to be used as an estimate of path length based on the geometric similarity, as measured by the Hausdorff distance, of the IMF to the original data vector. However, we presume that not only does the method occasionally select an erroneous IMF (IMF 1 for example) but it also reasons that in some cases more than one IMF could represent the pattern of erosion and deposition in the DoD and thereby the characteristic path length. In the flume experiment, the VMD-HD method selected the longest wavelength, IMF 5, 74% of the time and IMF 4, 24% of the time. There was only one instance in which IMF 1 was selected and neither IMF 2 or 3 were ever selected. Likewise, IMF 5 was selected for all three bars in the San Juan River dataset. This result agrees with observations from the signal processing literature wherein the lower frequency (in our case wavelength) IMFs (4 and 5) are thought to represent the true signal whereas the higher frequency (shorter wavelength) IMFs are attributed to noise (Boudraa et al., 2005). In our case we can verify visually that IMF 5 is most likely representative of the path length by tracing the path from erosional site to depositional site within the DoD using the manual method (Fig. 3 & 8).

https://doi.org/10.5194/egusphere-2023-1186
Preprint. Discussion started: 14 June 2023

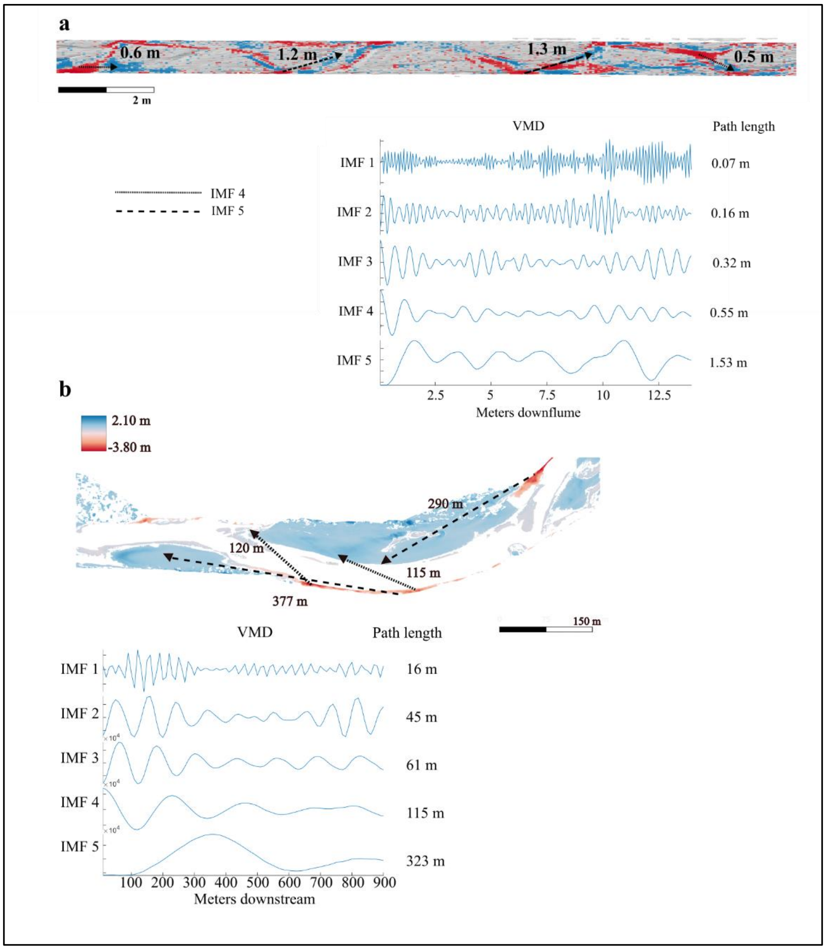

Figure 8: DoD with arrows showing possible path lengths between areas of erosion (red) to deposition (blue) corresponding to both IMF 4 and IMF 5. The VMD breakdown including all IMFs and the corresponding path lengths are shown for an experimental run from the 1.5 l discharge (a) and bar 15 from the San Juan River (b).

We also see shorter path lengths in the DoDs that may correspond to IMF 4 (Fig. 8). The method we present here to select one of the IMFs to represent the periodicity is convenient for assigning a characteristic path length to be used in sediment transport calculations. However, we recognize that in reality there is not one path length but rather a distribution. The path length-based method for calculating sediment transport necessitates that a single path length be selected and this is surely an oversimplification of reality. Encouragingly, the flume experiment shows that by using the VMD-HD method to select the path length, we are able to reasonably approximate sediment transport at the lower discharges (Fig. 6) even with an occasional erroneous result (i.e., IMF 1). However, when applying this method to a real case study, like that of the San Juan River, it is important to consider if the results make sense given what is known about the channel and the time and magnitude of flood events between surveys, potentially taking into account both IMF 4 and IMF 5 to generate a range of plausible transport.

The periodicity we extract from the DoDs as an estimate of path length corresponds to previous observations of preferential particle deposition at specific morphological units and relationships to channel morphology (Beechie, 2001;

https://doi.org/10.5194/egusphere-2023-1186
Preprint. Discussion started: 14 June 2023

Kasprak et al., 2015; Pyrce and Ashmore, 2003b). In the San Juan River study, our estimates aligned closely with the secondary modes in the particle path length distributions (Fig. 7) consistent with observations that at channel forming flows, particle path lengths tend to be bi or multimodal with secondary modes corresponding to the location of bars (Pyrce and Ashmore, 2003b). This preliminary result should be further examined with additional field data in multiple channel types.

We expected that the path length in more complex channels such as braided configurations would be more difficult to estimate due to the possibility of multiple path lengths active at different flow stages. In this study both the flume experiment and the field study exhibited a wandering morphology although in the flume experiment, the channel began to simplify at higher discharges. This is likely due to the inability of the channel to widen in response to the increase in discharge. Further, path length estimates did not change significantly between the discharges whereas the erosion volume increases with discharge, and that, as mentioned previously, potentially contributed to the underestimation of sediment flux at the higher discharges. Additionally, at the 1.5 l/s, and 2 l/s discharges, the patches of erosion and deposition began to overlap, therefore, the wavelike pattern from areas of erosion to deposition represented by the IMF 5 vector became flattened (Fig. 3). Further, when multiple channels are present and active, it may be beneficial to segregate the DoD, treating each channel as a separate system and generate multiple path length estimations. Further investigations are needed in the lab and in the field to propose robust methodologies to assess realistic ranges of path lengths from DoD for varying river patterns.

5.2 DoD related uncertainties

Any application of the morphological method using DoDs is sensitive to the error thresholding method used due to the way in which different thresholding techniques influence both the volumes of erosion and deposition as well as their spatial patterning (Brasington et al., 2003; Wheaton, 2008; Wheaton et al., 2010; Vericat et al., 2017). Because our method relies on the spacing between areas of erosion and deposition which is related to the size of the patches as well as which patches are detected, we considered that thresholding techniques could greatly affect the estimates of path length. We tested this hypothesis by applying the method to both the raw and filtered DoDs for the Trento flume experiment and found that while the volumes of erosion and deposition were lower after thresholding as expected ($p<0.001$), the path length estimates were not significantly different ($p>0.05$) (Appendix Table A1). While the thresholding here did not affect the path length estimates, we might imagine a scenario in which an entire area of erosion or deposition is removed through aggressive thresholding techniques, thereby potentially affecting the path length estimates and therefore caution that appropriate thresholding is important for the application of this method and the morphological method in general.

The time between surveys is of equal importance to the path length in the estimation of virtual velocity Eq. (2) and in the field can be highly uncertain due to poor availability of hydrologic data and/or the uncertainty of estimating the onset of transport based on a critical shear stress. Further, as time between surveys increases, so too does the probability of compensating erosion and deposition which can affect both the volumes of erosion and deposition and the topographic signatures (Lindsay and Ashmore, 2002; Vericat et al., 2017) necessary for VMD-HD method. We tested how the time between surveys might affect both the volumes of erosion and deposition and our path length estimates by differencing DEMs not every time step but between two, three, and four timesteps, each time step being one of the nine runs in the lab of phase 3 (see method). Not surprisingly the volume of erosion and deposition increased significantly with increasing time between surveys with the largest increase between the 1st timestep and 2nd timestep (Fig. 9). The path length estimates did not increase significantly for any of the discharges (Fig. 9c) indicating that the path length

https://doi.org/10.5194/egusphere-2023-1186
Preprint. Discussion started: 14 June 2023

estimate is stable, likely because, as already noted, the spacing of erosion and deposition is related to the position of erosional and depositional features which do not change much in a confined experiment. When both of these parameters are used in the sediment transport calculations and normalized by the increased time between surveys, we found no statistically significant difference between the estimates (Fig. 9d). However, though not statistically significant, there is an apparent decreasing trend in the sediment flux with the increased time between surveys, especially for the 2 l/s discharge that may indicate compensation (Fig. 9d). Despite the apparent trend at the highest discharge this is a promising result in that even by increasing the time interval by a factor of 4 we are still able to estimate sediment transport reasonably at the lower discharges. In the field there are often multiple flood events of differing magnitude in the year between surveys as was the case with the San Juan River study (McQueen et al., 2021). Although there were five flood events of differing magnitudes between the San Juan River surveys, we were still able to estimate path lengths corresponding to the RFID tracer data with an error of less than 30% (Fig. 7).

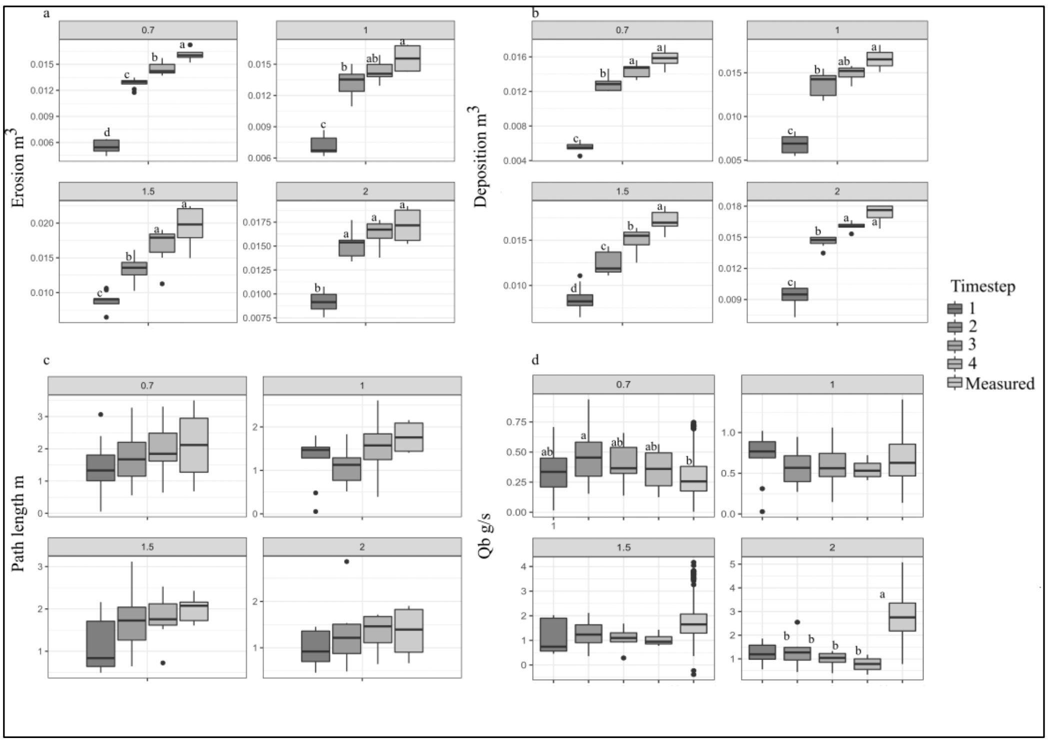

Figure 9: (a) Erosion measured from the flume experiments for each discharge and each timestep (b) deposition (c) path length estimates using VMD-HD method (d) sediment flux estimated using VMD-HD method and measured. Significant post-hoc Tukey results are denoted by letters a-d (α=0.05).

5.3 Applicability of the method

When evaluating the efficacy of our proposed method it is important to keep in mind the uncertainty of even direct measurement of sediment transport. The spatial and temporal frequency required to overcome the noise of measurement uncertainty (i.e., achieve an acceptable signal to noise ratio) in some cases can require sub-daily monitoring with precise equipment (Grams et al., 2019). The variability of sediment transport measurements in the flume study ranged from a standard deviation of approximately 30% to over 50% of the averaged flux (Fig. 3). Given this high variability, our reach scale averages were not significantly different from the measured averages for the 0.7 l/s and 1 l/s discharges

https://doi.org/10.5194/egusphere-2023-1186
Preprint. Discussion started: 14 June 2023

(Fig. 6). Further, our method produced path length estimates which correspond to the distance between erosional and depositional sites on the DoD in both the flumes and field (Fig. 7).

In the flume experiment, we found that the VMD-HD method performed better at the lower discharges of 0.7 l/s and 1 l/s but significantly underestimated the sediment transport at the 1.5 l/s and 2 l/s discharges (Fig. 6). In Sect. 5.1 we discussed that this underestimation is likely due to our limitations in the deriving realistic path lengths from DoDs. The underestimation at higher discharges could be related to the amount of morphological change relative to the sediment transport. Recently, Booker and Eaton (2022) quantitatively explored the link between sediment transport and morphology and proposed an index to represent the intuitive notion that as sediment transport increases relative to morphological change, the processes become decoupled and inferences from one to another become more difficult. They developed a 'throughput index' which is the ratio between sediment flux and morphological change and represents how much sediment moves through a reach without leaving a topographic signature of equal magnitude. Therefore, the ratio represents how well the flux is represented morphologically with the ratio approaching 1 when all of the flux is shown as morphological change and exceeding 1 when there is transport without equivalent morphological change. In our case the flume experiments were confined, therefore, as discharge increased the channel was not able to widen and deform laterally potentially causing the sediment to move through the flume without leaving an equivalent topographic signature. To explore the applicability of the method proposed we calculated the morphological active width by counting the percentage of pixels in the DoD that showed topographic change after filtering (we applied this metric only for the flume experiments since the San Jose DoDs do not include the submerged part of the channel). The morphological active width increased with discharge as expected and was positively correlated with the error of our estimates (Fig. 10). We found a strong exponential relationship between the percent of the flume that was active and the error of our estimates (R^2 =0.98, $p<0.01$) (Fig. 10). This result exposes a limitation of the morphological method in general and our application specifically, that is, confined channels with high transport relative to morphological change are likely poor candidates for the morphological method as inferences between changes in morphology and sediment transport become decoupled. Further applications of this method in the field and in the lab could identify a potential threshold defined by the throughput index (Booker and Eaton, 2022) or the morphological active width described in this study. The advantage of using the morphological active width as opposed to the throughput index is that it can be determined from the DoD without direct sediment transport measurements.

https://doi.org/10.5194/egusphere-2023-1186
Preprint. Discussion started: 14 June 2023

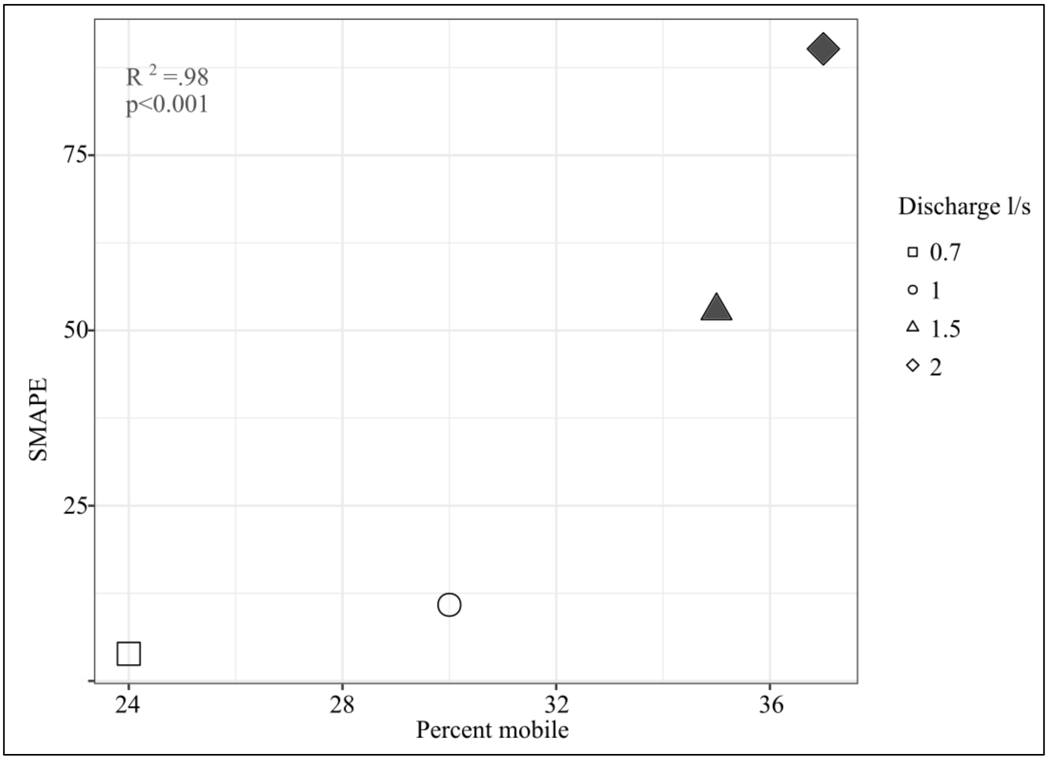

Figure 10: Symmetrical mean absolute percent error (SMAPE) between estimated and measured flux in the flume experiments vs the percentage of the DoD showing morphological change. Different discharges are denoted by shape. Filled shapes are where the sediment transport was significantly underestimated (α=0.05). R^2 and p value from exponential regression is shown.

6 Conclusion

The feasibility of estimating sediment flux using the morphological method has increased dramatically with the advent of high-resolution topography but has thus far been limited by the high labor demand of acquiring estimates of path length or the uncertainty of defining zero or known flux boundary. Given the observed connections between morphology and path length at channel forming flows, we hypothesized that the pattern of erosion and deposition can be a proxy for particle path length in gravel bed rivers. We applied tools from signal processing to quantify this periodicity and found that our method provides estimates path length within 30% of measured tracer data and corresponds to the spacing of erosion and deposition visible on the DoD. Further, our method provides estimates of path length coherent with channel morphology and previous observations of preferential particle deposition at given channel units, specifically bar heads and margins. When extended to calculate sediment flux our estimates were not significantly different from the measured average at low discharges. Importantly we found that limits arise where discharge increases in confined channels and sediment transport becomes decoupled from morphological changes. Our method provides a reasonable estimation of path length based solely on remotely sensed data and a novel method to estimate sediment fluxes associated with specific channel morphological processes through DoD interpretation.

Appendix A

Table 1A. Results from filtered vs raw DoDs from the flume experiments.

https://doi.org/10.5194/egusphere-2023-1186
Preprint. Discussion started: 14 June 2023

Discharge	Path length raw (m)	Path length filtered (m)	Qb estimated raw(g/s)	Qb estimated filtered (g/s)	Erosion raw (m3)	Deposition raw(m3)	Erosion filtered (m3)	Deposition filtered (m3)
0.7	1.773259	1.307314	0.689433	0.302282	0.009159	0.008549	0.005447	0.005563
0.7	0.795361	0.754067	0.29032	0.142154	0.008599	0.008908	0.004441	0.004537
0.7	3.046668	3.064947	1.199591	0.707274	0.009275	0.009918	0.005436	0.005387
0.7	2.535835	2.396349	0.968185	0.510259	0.008994	0.009598	0.005016	0.005359
0.7	2.295464	0.054816	1.013183	0.014801	0.010397	0.010241	0.006361	0.006194
0.7	0.871326	1.093539	0.346255	0.232138	0.009361	0.009446	0.005001	0.005344
0.7	1.566474	1.610973	0.699181	0.429163	0.010514	0.010212	0.006275	0.006408
0.7	1.244291	1.348844	0.564266	0.368507	0.010683	0.009538	0.006436	0.00574
1	1.24835	1.40561	1.038306	0.88725	0.010422	0.010825	0.007909	0.007682
1	1.365147	0.481025	1.276647	0.310621	0.011718	0.011387	0.008091	0.00773
1	1.247054	1.47142	1.096304	1.020008	0.011015	0.01074	0.008686	0.008282
1	1.228217	1.801574	1.179758	0.998633	0.012036	0.011354	0.006946	0.007335
1	1.479481	1.593984	1.46079	0.837967	0.012372	0.012056	0.006587	0.00651
1	1.829563	1.532486	1.573845	0.767802	0.010779	0.011239	0.006278	0.005849
1	1.537466	1.524962	1.265276	0.753475	0.010312	0.01053	0.006191	0.005744
1	1.513476	1.285303	1.214192	0.688794	0.010052	0.009902	0.006715	0.005483
2	1.406256	1.401221	2.526716	1.855525	0.013508	0.013539	0.009956	0.009756
2	0.908098	0.918657	1.582438	1.193736	0.013101	0.013743	0.009769	0.010142
2	1.258225	1.359801	2.048964	1.578538	0.012243	0.013183	0.008727	0.009491
2	1.127641	1.256842	1.665162	1.265188	0.011102	0.011877	0.007568	0.008187
2	0.055676	1.453594	0.088489	1.610442	0.011949	0.010872	0.008329	0.0073
2	0.464373	0.461198	0.776033	0.561071	0.012564	0.012399	0.009146	0.00892
2	1.31982	0.826137	2.035505	1.182625	0.011595	0.013636	0.010762	0.009229
2	0.712963	0.65993	1.29628	0.740195	0.013669	0.014229	0.008432	0.010081

Summary

Discharge	Erosion	Deposition	Path Length	Qb

0.7	**p<0.001****	**p<0.001****	**p>0.05**	**p<0.05***
1	**p<0.001****	**p<0.001****	**p>0.05**	**p<0.05***
2	**p<0.001****	**p<0.001****	**p>0.05**	**p>0.05**

***p-values from student's t test between raw and filtered data**

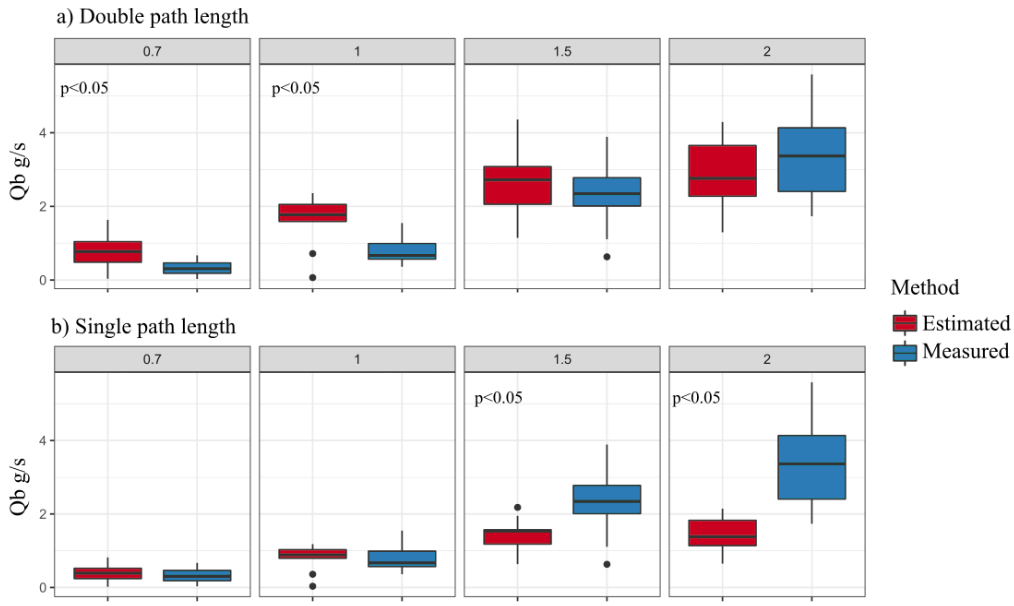

Figure 1A. Sediment transport calculated using the single path length estimate from the VMD-HD method (b) and doubling the path length estimate (a). Estimated flux is red and measured flux is blue. Significant p values are shown.

Code availability

Data and code are available upon request form the corresponding author.

Author contribution

LC, SB, WB and NS conceptualized the study. EP and WB preformed the experiments. LC, SB and WB designed the method. LC performed statistical analysis. LC, EP, and WB wrote the manuscript. LC, SB, EP, WB, and NS edited the manuscript.

Competing interests

The authors declare they have no competing interests.

Financial support

This work was supported by the CARIPARO foundation and the University of Padova.

References

Ashmore, P.E., Church, M. Sediment transport and river morphology: a paradigm for study. Gravel-bed Rivers in the Environment, Hey, R.D., Bathurst, J.C., Thorne, C.R. (eds). Wiley: Chichester; 115–148. 1998.

Beechie, T. J.: Empirical predictors of annual bed load travel distance, and implications for salmonid habitat restoration and protection, Earth Surf. Process. Landf., 26, 1025–1034, https://doi.org/10.1002/esp.251, 2001.

https://doi.org/10.5194/egusphere-2023-1186
Preprint. Discussion started: 14 June 2023

Booker, W. H. and Eaton, B. C.: Morphodynamic styles: characterising the behaviour of gravel-bed rivers using a novel, quantitative index, Earth Surf. Dyn., 10, 247–260, https://doi.org/10.5194/esurf-10-247-2022, 2022.

Boudraa, A.-O., Cexus, J.-C., and Saidi, Z.: EMD-Based Signal Noise Reduction, Signal Process., 1, 2005.

Brasington, J., Langham, J., and Rumsby, B.: Methodological sensitivity of morphometric estimates of coarse fluvial sediment transport, Geomorphology, 53, 299–316, https://doi.org/10.1016/S0169-555X(02)00320-3, 2003.

Brenna, A., Surian, N., and Mao, L.: Virtual Velocity Approach for Estimating Bed Material Transport in Gravel-Bed Rivers: Key Factors and Significance, Water Resour. Res., 55, 1651–1674, https://doi.org/10.1029/2018WR023556, 2019.

Dragomiretskiy, K. and Zosso, D.: Variational Mode Decomposition, IEEE Trans. Signal Process., 62, 531–544, https://doi.org/10.1109/TSP.2013.2288675, 2014.

Garcia Lugo, G. A., Bertoldi, W., Henshaw, A. J., and Gurnell, A. M.: The effect of lateral confinement on gravel bed river morphology, Water Resour. Res., 51, 7145–7158, https://doi.org/10.1002/2015WR017081, 2015.

Grams, P. E., Topping, D. J., Schmidt, J. C., Hazel Jr., J. E., and Kaplinski, M.: Linking morphodynamic response with sediment mass balance on the Colorado River in Marble Canyon: Issues of scale, geomorphic setting, and sampling design, J. Geophys. Res. Earth Surf., 118, 361–381, https://doi.org/10.1002/jgrf.20050, 2013.

Grams, P. E., Buscombe, D., Topping, D. J., Kaplinski, M., and Hazel, J. E.: How many measurements are required to construct an accurate sand budget in a large river? Insights from analyses of signal and noise, Earth Surf. Process. Landf., 44, 160–178, https://doi.org/10.1002/esp.4489, 2019.

Hassan, M. A. and Bradley, D. N.: Geomorphic Controls on Tracer Particle Dispersion in Gravel-Bed Rivers, in: Gravel-Bed Rivers, John Wiley & Sons, Ltd, 159–184, https://doi.org/10.1002/9781118971437.ch6, 2017.

Hassan, M. A., Church, M., and Schick, A. P.: Distance of movement of coarse particles in gravel bed streams, Water Resour. Res., 27, 503–511, https://doi.org/10.1029/90WR02762, 1991.

Hoey, T.: Temporal variations in bedload transport rates and sediment storage in gravel-bed rivers, Prog. Phys. Geogr. Earth Environ., 16, 319–338, https://doi.org/10.1177/030913339201600303, 1992.

Huang, N., Chen, H., Cai, G., Fang, L., and Wang, Y.: Mechanical Fault Diagnosis of High Voltage Circuit Breakers Based on Variational Mode Decomposition and Multi-Layer Classifier, Sensors, 16, 1887, https://doi.org/10.3390/s16111887, 2016.

Hundey, E. J. and Ashmore, P. E.: Length scale of braided river morphology: Length Scale of Braided River Morphology, Water Resour. Res., 45, https://doi.org/10.1029/2008WR007521, 2009.

Kasprak, A., Wheaton, J. M., Ashmore, P. E., Hensleigh, J. W., and Peirce, S.: The relationship between particle travel distance and channel morphology: results from physical models of braided rivers., J. Geophys. Res. Earth Surf., 120, 55–74, 2015.

Liébault, F., Bellot, H., Chapuis, M., Klotz, S., and Deschâtres, M.: Bedload tracing in a high-sediment-load mountain stream, Earth Surf. Process. Landf., 37, 385–399, https://doi.org/10.1002/esp.2245, 2012.

Lindsay, J. B. and Ashmore, P. E.: The effects of survey frequency on estimates of scour and fill in a braided river model, Earth Surf. Process. Landf., 27, 27–43, https://doi.org/10.1002/esp.282, 2002.

Ma, W., Yin, S., Jiang, C., and Zhang, Y.: Variational mode decomposition denoising combined with the Hausdorff distance, Rev. Sci. Instrum., 88, 035109, https://doi.org/10.1063/1.4978029, 2017.

McDowell, C. and Hassan, M. A.: The influence of channel morphology on bedload path lengths: Insights from a survival process model, Earth Surf. Process. Landf., 45, 2982–2997, https://doi.org/10.1002/esp.4946, 2020.

McDowell, C., Gaeuman, D., and Hassan, M. A.: Linkages between bedload displacements and topographic change, Earth Surf. Process. Landf., 46, 3127–3142, https://doi.org/10.1002/esp.5221, 2021.

McLean, D. G. and Church, M.: Sediment transport along lower Fraser River: 2. Estimates based on the long-term gravel budget, Water Resour. Res., 35, 2549–2559, https://doi.org/10.1029/1999WR900102, 1999.

https://doi.org/10.5194/egusphere-2023-1186
Preprint. Discussion started: 14 June 2023

McQueen, R., Ashmore, P., Millard, T., and Goeller, N.: Bed Particle Displacements and Morphological Development in a Wandering Gravel-Bed River, Water Resour. Res., 57, https://doi.org/10.1029/2020WR027850, 2021.

Pyrce, R. and Ashmore, P.: The relation between particle path length distributions and channel morphology in gravel-bed streams: A synthesis, Geomorphology, 56, 167–187, https://doi.org/10.1016/S0169-555X(03)00077-1, 2003a.

Pyrce, R. S. and Ashmore, P. E.: Particle path length distributions in meandering gravel-bed streams: results from physical models, Earth Surf. Process. Landf., 28, 951–966, https://doi.org/10.1002/esp.498, 2003b.

Roux, C., Alber, A., Bertrand, M., Vaudor, L., and Piégay, H.: “FluvialCorridor”: A new ArcGIS toolbox package for multiscale riverscape exploration, Geomorphology, 242, 29–37, https://doi.org/10.1016/j.geomorph.2014.04.018, 2015.

Upadhyay, A. and Pachori, R. B.: Instantaneous voiced/non-voiced detection in speech signals based on variational mode decomposition, J. Frankl. Inst., 352, 2679–2707, https://doi.org/10.1016/j.jfranklin.2015.04.001, 2015.

Vázquez-Tarrío, D., Recking, A., Liébault, F., Tal, M., and Menéndez-Duarte, R.: Particle transport in gravel-bed rivers: Revisiting passive tracer data: Particle transport in gravel-bed rivers, Earth Surf. Process. Landf., 44, 112–128, https://doi.org/10.1002/esp.4484, 2019.

Vericat, D., Church, M., and Batalla, R. J.: Bed load bias: Comparison of measurements obtained using two (76 and 152 mm) Helley-Smith samplers in a gravel bed river, Water Resour. Res., 42, https://doi.org/10.1029/2005WR004025, 2006.

Vericat, D., Wheaton, J. M., and Brasington, J.: Revisiting the Morphological Approach, in: Gravel-Bed Rivers, John Wiley & Sons, Ltd, 121–158, https://doi.org/10.1002/9781118971437.ch5, 2017.

Wheaton, J. M.: Uncertainity in morphological sediment budgeting of rivers, phd, University of Southampton, 2008.

Wheaton, J. M., Brasington, J., Darby, S. E., and Sear, D. A.: Accounting for uncertainty in DEMs from repeat topographic surveys: improved sediment budgets, Earth Surf. Process. Landf., 35, 136–156, https://doi.org/10.1002/esp.1886, 2010.